JOURNAL OF SOLID STATE CHEMISTRY 94, 220–226 (1991)

Composition and Structure of Phases Formed in the Process of Hydrated Antimony Pentoxide Thermolysis

DMITRI KLESTCHOV

Research Institute of Inorganic Pigments and Coatings, USSR

VLADIMIR BURMISTROV

City of Chelyabinsk University, USSR

AVRAAM SHEINKMAN

City of Chelyabinsk University, USSR

AND RAFAEL PLETNEV

Institute of Chemistry of the Academy of Sciences (the Ural Department), USSR

Received November 1, 1990; in revised form May 1, 1991

The composition and structure of phases formed in the thermolysis of hydrated antimony pentoxide (HAP) have been studied by means of X-ray diffraction, isothermal thermogravimetric, volumetric, and NMR methods. It has been shown that (a) the HAP thermolysis at 400–1110 K proceeds in four steps: at each step a phase of specific composition is formed (P_i-phases: $i = 2$–5). The P_5-phase, composition Sb_6O_{13}, is known. Phases P_2, P_3, and P_4 have been identified in the present study. (b) The HAP $\rightarrow P_2$ and $P_2 \rightarrow P_3$ transformations are accompanied only by dehydration; the $P_5 \rightarrow Sb_2O_4$ transformation is accompanied only by reduction processes; the $P_3 \rightarrow P_4$ and $P_4 \rightarrow P_5$ transformations are accompanied by both dehydration and reduction. (c) The HAP of formula $Sb_2O_5 \cdot nH_2O$, with $2 \leq n \leq 4$, is a phase of variable composition, ranging from $Sb_2O_5 \cdot 2H_2O$ to $Sb_2O_5 \cdot 4H_2O$. (d) The protons in HAP are present in the form of hydrogen and/or hydronium ions, as well as water molecules of crystallization; in P_i-phases ($i = 2$–4) they exist only in the form of hydrogen ions. The H^+ and $(H_2O)H^+$ ions are statistically distributed over positions 16*d*, while antimony and oxygen atoms and water molecules of crystallization occupy positions 16*c*, 48*f*, and 8*b*, respectively. © 1991 Academic Press, Inc.

Introduction

Hydrated antimony pentoxide (HAP) or "antimonic acid" is a cation-exchange material (*1, 2*) characterized by a high ion-exchange capacity (up to 5 meq/g) (*2–4*) and selectivity to mono- (Ag^+, Na^+) and divalent (Hg^{2+}, Sr^{2+}) cations, with radii close to 1 Å (*5*). HAP has an empirical formula $Sb_2O_5 \cdot nH_2O$; n depends on the preparation method and varies widely from approximately 30 for amorphous samples (*1*) to 3–4 and even 1 for crystalline samples (*2, 4, 6*).

Upon heating HAP at 330–1200 K the de-

0022-4596/91 $3.00

hydration is accompanied by a reduction of part of the Sb(V) cations to Sb(III) (*1, 2, 7–13*). The end-product of HAP thermolysis in air at temperatures higher than 1100 K is a mixture of phases α- and β-Sb_2O_4 (*1, 2, 6–13*). The phase α-Sb_2O_4 is orthorhombic (space group symmetry $Pna2_1$; a = 5.436 Å; b = 4.810 Å; c = 11.76 Å (*14*)), while β-Sb_2O_5 is monoclinic (space group symmetry $C2/c$; a = 12.060 Å; b = 4.834 Å; c = 5.383 Å; β = 104.35 (*15*)). The sequence of HAP transformations and the composition of the intermediate phases being formed are still open to discussion.

According to (*1, 7*) the thermolysis of HAP involves two steps in which the formation of anhydrous Sb_2O_5 (290–670 K) and Sb_6O_{13} (670–1100 K) takes place. In (*8–10*) the formation of Sb_2O_5 during thermolysis of HAP in air is questioned. According to data presented in (*8*) the thermolysis of HAP is accomplished in three steps, with Sb_3O_6OH being formed at 620–890 K. The formation of Sb_3O_6OH is also discussed in (*11*), but not confirmed by the data of (*9*), the authors of which state the impossibility of obtaining compounds of reproducible composition between 400 and 1000 K.

The object of the present work is to conduct a more accurate study of the sequential steps of HAP thermolysis, to characterize the composition and structure of phases being formed, and to determine the temperature intervals of their stability.

Experimental

Hydrated antimony pentoxide was prepared from a 10% hydrochloric acid solution of antimony tetrachloride (with an $SbCl_3$: HCl ratio of 1 : 2) oxidized by means of a 5% hydrogen peroxide solution at 300 K; all reagents were of analytical purity. No precipitate was formed during oxidation. The solution obtained was hydrolyzed in a large amount of water at 300 K. The precipitate was aged in the mother liquor for 2 days at 300 K and at 335 K for two more days, washed in distilled water until free of chloride ions, dried to constant weight at 320–350 K, and placed in a water-filled glass container to attain the equilibrium composition.

The sample prepared as described above is a white powder of composition $Sb_2O_5 \cdot 4.05H_2O$ (as determined by thermogravimetric and volumetric analysis); the crystal size was approximately 300 Å (by X-ray analysis).

The substitution of counterions in the HAP and in phases formed during thermolysis by silver cations was conducted in a 0.1 N solution of $AgNO_3$ of analytical purity under static conditions, with a mass ratio of the solid to liquid of 1 : 100. The contact time of the HAP with the solution was 48 hr. The ion-exchange capacity was evaluated by observing the change of the silver concentration in the solution.

In the course of the present work several methods have been used, including isothermal thermogravimetry, derivatography (Paulic–Erday derivatograph; sample heating rate about 10 K/min), mass spectrophotometry (using an MX-130 mass spectrophotometer equipped with a device for programmed heating of the sample at a constant rate of about 5 K/min), isothermal volumetric analysis (specially designed volumeter capable of measuring the volume of O_2 liberated during HAP thermolysis with an accuracy no lower than 3.5 rel%), X-ray diffraction analysis (DRON-3 X-ray diffractometer with filtered Cu$K\alpha$ radiation), proton magnetic resonance (^{1}H NMR) spectrography (NMR-radiospectrometer; f_0 = 80 mHz; modulation amplitude from 0.1 to 1.0 Oe).

The lattice parameters a of the unit cell of the HAP and its thermolysis products were determined relative to a NaCl standard, using the (10, 6, 2) and (12, 0, 0) diffraction lines of HAP. The error of the parameter a evaluation did not exceed 0.05%.

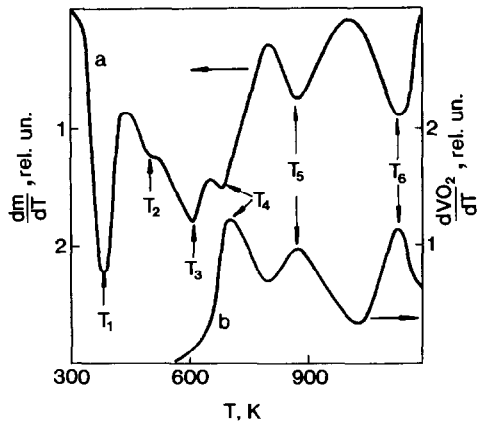

FIG. 1. Temperature dependence of the sample mass $\frac{dm}{dT}$ (a) and of the liberated oxygen mass $\frac{dVO_2}{dT}$ (b) during HAP thermolysis.

Results and Discussion

Stages of HAP thermolysis. The thermogravimetric curve of HAP thermolysis is similar to those described in the literature (*8, 9*). The total sample mass loss through the interval 300–1170 K amounted to 28.6% of the sample mass at 1170 K. On the derivatographic curve (Fig. 1, curve a) six extrema are indicated at T_i (i = 1–6) values of 382, 543, 603, 683, 878, and 1140 K. Oxygen is liberated at temperatures higher than 600 K, but not in one continuous reaction (Fig. 1, curve b): three maxima of the oxygen evolution are registered close to 670, 870, and 1150 K, which agrees satisfactorily with the extrema on the derivatographic curve.

X-ray diffraction analysis of equilibrium products obtained at temperatures close to T_i shows that the end-product of the thermolysis is a mixture of α- and β-Sb_2O_4. The initial HAP X-ray patterns and those of intermediate thermolysis products obtained at 300–1000 K include similar sets of diffraction maxima assignable to a cubic symmetry (space group $Fd3m$), which agrees with data presented in numerous other papers (*1, 2, 4, 6, 11–13*). It is also established that during constant heating the a parameter of the unit cell undergoes changes (Fig. 2, curve b), testifying to the step-by-step character of HAP thermolysis.

The kinetic curves of sample weight loss and variation of the parameter a of the unit cell at 370–1100 K, as well as the Δm_{O_2} curve (liberated oxygen at 600–1100 K) are sigmoidal and are characterized by a short (less than 5 min) induction period. With an increase in thermal treatment time, $\Delta m(\tau)$, $a(\tau)$, and $\Delta m_{O_2}(\tau)$ tend to constant values for a given temperature. Consequently, under prolonged isothermal aging, the decomposition products reach an equilibrium state. Allowing for experimental error, the relative variations Δm,a, and Δm_{O_2} at temperatures assignable to a fixed thermolysis step (except step 1 at 300–370 K for Δm and a) coincide. However, they differ from those obtained at other thermolysis steps; this testifies to the step-by-step nature of the temperature dependence of the sample weight loss, oxygen evolution, and parameter a variation. It follows from Fig. 2 that temperatures where abrupt variations Δm take place (Fig. 2, curve a) satisfactorily coincide with those determined from the a parameter

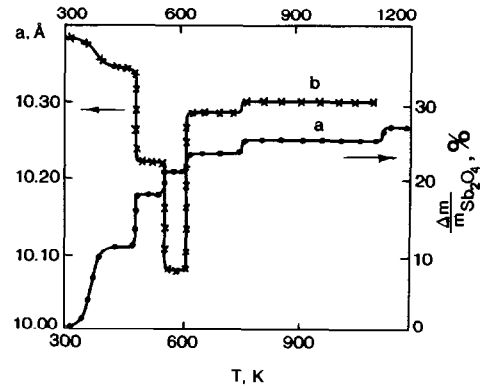

FIG. 2. Temperature dependence of the equilibrium sample mass $\frac{\Delta m}{m}$ (a) and the parameter a of the unit cell of HAP thermolysis products (b).

and from the mass temperature dependence of liberated oxygen. Therefore, it is concluded that all these characteristics are interrelated and are based on the same processes.

On the basis of isothermal thermogravimetry, volumetry, and X-ray analysis it is concluded that the equilibrium products of HAP thermolysis obtained at stages 2–5 have distinct compositions and crystal structures and therefore are individual compounds (phases). The phases formed at steps 2 to 5 of HAP thermolysis will be referred to as P_i-phases (i = 2–5). From temperature variations of the sample mass, liberated oxygen mass, and parameter a of the unit cell we have determined the formation (T_i^{min}) and decomposition (T_i^{max}) boundary temperatures of the P_i phases (see Table I).

State of protons in HAP and P_i phases. The ^1H NMR spectrum of HAP with the empirical formula $Sb_2O_5,4H_2O$ (recording temperature 125 K) (Fig. 3, curve a) has a complicated shape; there are three components with ΔH_1 = 4.8 G, ΔH_2 = 12.0 G, and ΔH_3 = 19.0 G (the second moment S_2 = 27.8 G^2). The first and third maxima are absent from the NMR spectra of the Ag^+-exchanged samples (Fig. 3, curve b), while the second does not undergo significant changes. Therefore, the second constituent of the spectrum is related to protons not involved in the cation exchange. Data from Ref. (*16*) show that the component ΔH_2 = 12.0 G is related to water of crystallization with an interprotonic distance r_{H-H} = 1.62 Å and an intermolecular interaction value β = 2.0 G^2.

The first and the third components of the NMR spectrum are very likely related to the counterion. The counterion spectrum obtained graphically by means of substraction of the HAP spectrum and that of the Ag^+-form of HAP (Fig. 3, curve e) has an appearance typical of a three-spin system (equilateral triangle) with parameters r_{H-H} and β equal to 1.70 Å and 1.8 G^2, respectively (as calculated according to (*17*)). The integral intensity ratio of the HAP and its Ag^+-derivative NMR spectrum was 3 : 1. It is concluded that in $Sb_2O_5 \cdot 4H_2O$ six out of eight protons are included in three-spin proton groups, and the remainder in water molecules of crystallization.

The ^1H NMR spectrum (recorded at 125 K) of HAP with composition $Sb_2O_5 \cdot 2H_2O$ is close to that of the initial HAP (Fig. 3, curve c) with one significant difference: the intensity of the first component is substantially higher than that of the second and third components. This leads to a decrease of the second moment S_2 to 19.0 G^2 and suggests that there are now some relatively isolated protons in the sample at 125 K, in addition to two- and three-spin protonic configurations. We also observed a plateau at 210–230 K when plotting S_2 versus the temperature (not shown here); the corresponding spectrum (Fig. 3, curve d) is a superposition of a singlet (ΔH = 3.0 G) and a doublet (ΔH = 10.0 G), with a 1 : 1 proton ratio. These results suggest that, with decreasing temperature, the mobility of the H_2O molecules freezes out and that three-spin proton groups are formed as a result of single protons locating on H_2O molecules at lower temperatures. Therefore, three-spin proton groups are not static (ion H_3O^+) but dynamic formations which can dissociate according to the probable reaction: $(H_2O)H^+ \rightleftarrows H_2O + H^+$.

The ^1H NMR spectra of the P_i-phases (i = 2–4) are represented by a singlet line with ΔH at 125 K equal to 4.0, 3.0, and 2.5 G, and the second moment S_2 equal to 7.0, 3.9, and 1.9 G^2, respectively. The corresponding P_i-phases of Ag^+-exchanged samples produce no NMR signal, which leads to the conclusion that all protons in the P_i-phases are in an equivalent state—that of hydrogen ions H^+. The P_5-phase does not produce an NMR signal. Therefore, protons are completely removed from the HAP structure only in the course of the P_4 to P_5 transformation.

TABLE I

COMPOSITION, STRUCTURAL FORMULAE, AND TEMPERATURE STABILITY REGION OF P_i-PHASES

Phase designation	$T_{P_i}^{min}$ (K)	$T_{P_i}^{max}$ (K)	$\Delta m/m_0^a$ (%)	$\Delta m/m_0^a$ (%)	Sb(III)/Sb(V) ratio	Phase composition	16d	16c	48f	8b
HAP	—	—	—	—	0	$Sb_2O_5\,4H_2O$	$16(H_2O)H^+$	16Sb(V)	48 O^{2-}	8 H_2O
	—	400	0–11.7	0	0	$Sb_2O_5\,nH_2O$ $(2 \le n \le 4)$	$(8n - 16)(H_2O)H^+ + (32 - 8n)H^+$	16Sb(V)	48 O^{2-}	8 H_2O
	400	470	0	0	0	$Sb_2O_5\,2H_2O$	$16H^+$	16Sb(V)	48 O^{2-}	8H_2O
P_2	480	540	7.3 ± 0.2	0	0	$H_{1.52}Sb_2O_{5.76}$	14H + 2Sb(V)	16Sb(V)	48 O^{2-}	4 O^{2-}
P_3	550	590	3.6 ± 0.1	0	0	$H_{0.38}Sb_2O_{5.195}$	4H + 4Sb(V)	16Sb(V)	48 O^{2-}	4 O^{2-}
P_4	600	770	2.3 ± 0.1	1.93 ± 0.07	0.24	$H_{0.19}Sb_2O_{4.69}$	2H + 4Sb(III) + 2Sb(V)	16Sb(V)	48 O^{2-}	4 O^{2-}
P_5	780	1100	1.7 ± 0.1	1.39 ± 0.05	0.50	$Sb_2O_{4.34}$	8Sb(III)	16Sb(V)	48 O^{2-}	4 O^{2-}
Sb_2O_4	1120	—	1.7 ± 0.1	1.78 ± 0.07	1.00	Sb_2O_4	—	—	—	—

[a] Sample mass variation and liberated oxygen mass variation are expressed relative to Sb_2O_4 mass.

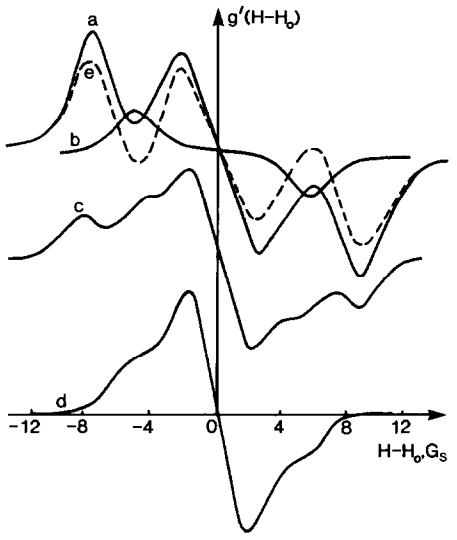

FIG. 3. First derivative G' $(H\text{-}H_0)$ of ^1H NMR spectra of HAP and of its Ag^+ ion-exchanged form. (a) HAP with composition $Sb_2O_5\,4.05H_2O$ (125 K); (b) Ag^+-form of HAP (125 K); (c, d) HAP compositions $Sb_2O_5\,2H_2O$ (125 K and 220 K, respectively). The dotted line (e) represents a three-spin proton group obtained by substraction of spectra a and b.

Composition of HAP and P_i-phases (i = 2–5). The composition of HAP and P_i-phases has been determined by weight loss and oxygen evolution at each thermolysis stage (see Table I). The oxygen loss at steps 4–6 of the HAP thermolysis accounts for 5.1 ± 0.1%, which coincides, within the error limits, with the theoretical value 5.19% for the $Sb_2O_5 \cdot 4H_2O \rightarrow Sb_2O_4$ transformation. Consequently, in the P_2- and P_3-phases all antimony ions are in the pentavalent state.

The P_5-phase, which is formed at 780–1110 K, has the composition $Sb_2O_{4.34}$ or Sb_6O_{13}, which agrees with numerous literature data (*1, 2, 6–9*).

The composition of the P_4-phase is $H_{0.18}Sb_2O_{4.69}$, with α an Sb(III) to Sb(V) ratio of 0.24. In (*8, 11*) the formation of Sb_3O_6OH was postulated for the same temperature interval, the Sb(III)/Sb(V) ratio be-

ing 0.5. The $P_4 \rightarrow P_5$ transformation would then be accompanied only by dehydration. However, the experimental data show that oxygen is liberated during the $P_4 \rightarrow P_5$ transformation and that the mass of the liberated oxygen constitutes about 80% of the total weight loss at step 5. This unambiguously testifies to a reduction process which accompanies the above-mentioned transformation.

The P_3-phase formed at 550–590 K has a composition of $H_{0.39}Sb_2O_{5.195}$, in contrast to (*1, 7*) where the formation of anhydrous antimony pentoxide was postulated. The NMR-signal and the P_3-phase ion-exchange properties clearly indicate the presence of hydrogen ions.

The composition of the P_2-phase is $H_{1.52}Sb_2O_{5.76}$. The NMR analysis shows that the compound contains hydrogen ions. Consequently, the HAP $\rightarrow$ P_2-phase transformation is accompanied by removal of water of crystallization from the structure, along with a redistribution of hydrogen ions.

During the HAP thermolysis at 300–470 K, the three-spin proton groups are destroyed and water is removed. Taking into account the monotonic HAP unit cell parameter variation with composition in the temperature range 300–370 K (Fig. 2, curves a and b), it is concluded that in this temperature interval HAP is a phase of variable composition $Sb_2O_5 \cdot nH_2O$, in the range $Sb_2O_5 \cdot 4H_2O$ and $Sb_2O_5 \cdot 2H_2O$. The exact composition depends on the experimental conditions, such as the ambient temperature and the relative humidity. This is probably the reason for the difference in *a*-values reported by different authors.

The HAP and P_i-phase structures. According to numerous reports (*1, 2, 4, 6, 8–12*), HAP and its thermolysis products have (up to 1100 K) a pyrochlore-type structure, space group $Fd3m$, structural formula $A_{16}B_{16}X_{18}X''_8$ (*18*). The framework of the pyrochlore-type structure consists of a three-dimensional network of BX_6^1-octahedra jointed along edges; the excess negative charge is compensated with mono-, di, and trivalent cations and X'' anions. *A, B, X,* and X'' are located in positions 16*d*, 16*c*, 48*f*, and 8*b* of the space group $Fd3m$, respectively (*16*).

According to NMR data the structural formula of HAP as a phase of variable composition $Sb_2O_5 \cdot nH_2O$ can be represented as $[(H_2O)H]_{8n-16}H_{32-8n}Sb_{16}O_{48} \cdot 8H_2O$ ($2 \leq n \leq 4$).

The H^+ and $(H_2O)H^+$ ions are statistically distributed over positions 16*d*, while antimony and oxygen atoms and water molecules of crystallization occupy positions 16*c*, 48*f*, and 8*b*, respectively.

As Table I shows HAP $\rightarrow$ P_2, and $P_i \rightarrow P_{i+1}$ (i = 2–4) transformations are accompanied by removal of hydrogen ions. Since hydrogen ions in HAP and P_i-phases play an important chemical role as pyrochlore-type structure stabilizers by neutralizing the network excess negative charge, a portion of the antimony ions must be transferred from position 16*c* to 16*d* during the above-mentioned transformations (*2, 9, 12, 13*). It is assumed in (*9*) that in the transition of Sb(V) ions to positions 16*d* they are reduced to the trivalent state. However, taking into consideration the results of volumetric studies, reduction processes take place only at temperatures higher than 600 K, and antimony ions in P_2- and P_3-phases remain in the highest oxidation state. The transition of antimony ions to positions 16*d*, with respect to their valency, explains the variation of the lattice parameter *a* of the P_i-phases with temperature (Fig. 2b). Because the ionic radius of Sb(V) is significantly (1.5 times) smaller than that of Sb(III) and that of $(H_2O)H^+$, the transition of Sb(V) to positions 16*d* should decrease the parameter *a* according to Vegard's law; this is indeed experimentally confirmed for the HAP–P_2–P_3 series. During the $P_3 \rightarrow P_4$ transformation Sb(V) ions in positions 16*d* are reduced to the trivalent state, which manifests itself in a sharp in-

crease of parameter a of the P_4-phase as compared to the P_3-phase.

As concerns the P_i-phase (i = 2–5) structures, the most complete study was made of the P_5-phase, e.g., Sb_6O_{13} (*9*). The authors of (*9*) believe the most probable distribution over the positions of space group $Fd3m$ to be

16*d*	16*c*	48*f*	8*b*
8Sb(III)	16Sb(V)	48 O^{2-}	4 O^{2-}

The structural formulae of the P_i-phases have been determined on the basis of empirical composition data (see Table I), taking into account the requirements of electroneutrality and assuming the absence of regular imperfections for compounds with the pyrochlore-type structure in positions 16*c* and 48*f*. In addition, it was assumed that the Sb ion number in positions 16*d* of P_i-phases (i = 2–5) changes in discrete steps of two.

Thus, HAP possesses the ideal pyrochlore-type structure, while the P_i-phases (i = 2–5) have derivative structures with systematic imperfections. A general rule makes itself manifest for compounds with defect pyrochlore-type structures: the occupancy coefficient in positions 16*d* and 8*b* can have only two discrete values: 1 and 0.5. This is probably a result of the imposition of crystal structure symmetry requirements.

Summary

1. Hydrated antimony pentoxide thermolysis conducted at 400–1100 K proceeds in four steps; at each of those steps a phase of specific composition is formed (P_i-phases, i = 2–5). The P_5-phase, composition Sb_6O_{13}, is known from the literature. Phases P_2, P_3, and P_4 were discovered in the present study.

2. The HAP → P_2 and P_2 → P_3 transformations are accompanied only by dehydration: the P_5 → Sb_2O_4 transformation is accompanied only by reduction processes: the P_3 → P_4 and P_4 → P_5 transformations are accompanied by both dehydration and reduction.

3. Hydrated antimony pentoxide of formula $Sb_2O_5 \cdot nH_2O$, with $2 \leq n \leq 4$, is a phase of variable composition, the extremities being $Sb_2O_5 \cdot 2H_2O$ and $Sb_2O_5 \cdot 4H_2O$.

4. Protons in HAP structure are present in the form of hydrogen ions and/or three-spin proton groups, e.g., hydronium ions, H_3O^+, or $(H_2O)H^+$, as well as in water molecules of crystallization while in the P_i-phases (i = 2–4) they are present only in the form of hydrogen ions.

References

1. M. Abe and T. Ito *Bull. Chem. Soc. Japan* **41,** 333 (1968).
2. F. A. Belinskaya and E. A. Militsina *Usp. Khim.* **49,** 1904 (1980).
3. J. Lefevre and F. Gaymard *Comp. Rendu.* **260,** 6911 (1965).
4. L. H. Beastle and D. J. Huys *Inorg. Nucl. Chem.* **30,** (1968).
5. M. Abe, M. Tsuji, and N. Kimura *Bull. Chem. Soc. Japan* **54,** 1300 (1981).
6. I. P. Olenkova and L. M. Plyasova *Zh. Strukt. Khim.* **19,** 1040 (1978).
7. A. Simon and E. Thaler *Z. Anorg. Allgem. Chem. B.* **161,** 113 (1927).
8. B. G. Novikov, E. L. Meterow, and F. A. Belynskaya *Zh. Neorg. Khim.* **20,** 1566 (1975).
9. D. J. Steart, O. Knop, C. Ayasse, and F. W. D. Woodhams *Canad. J. Chem.* **50,** 690 (1972).
10. D. G. Klestchov, A. A. Polyakov, A. V. Tolchev, V. A. Burmistrov, and G. V. Klestchov *Isv. Akad Nauk SSSR, Neorg. Mater.* **19,** 1505 (1983).
11. K. Dilstroem and A. Westgren *Z. Anorg. Allgem. Chem., B.* **235,** 153 (1937).
12. G. V. Klestchov, V. G. Trofimov, D. G. Klestchov, and A. I. Sheinkman, *Kristallografia* **21,** 832 (1976).
13. V. A. Burmistrov, D. G. Klestchov, V. N. Konev, and R. N. Pletnev, *Zh. Neorg. Khim.* **30,** 1959 (1985).
14. A. C. Skapski and D. Rogers *Chem. Commun.* **23,** 611 (1965).
15. D. Rogers and A. C. Skapski *Proc. Chem.*, Dec., 400 (1964).
16. G. E. Pake *J. Chem. Phys.* **16,** 372 (1948).
17. E. R. Andrew, and R. Berson *J. Chem. Phys.* **20,** 1159 (1950).
18. V. A. Yusupov *Kristallografia,* **3,** 99 (1958).